PERIODICO di MINERALOGIA
established in 1930

DIPARTIMENTO
DI SCIENZE DELLA TERRA

SAPIENZA
UNIVERSITÀ DI ROMA

An International Journal of
Mineralogy, Crystallography, Geochemistry,
Ore Deposits, Petrology, Volcanology
and applied topics on Environment, Archaeometry and Cultural Heritage

Pseudosection modelling of the Precambrian meta-pelites from the Poshtuk area, NW Iran

Adel Saki [1,*], Mirmohammad Miri [1], Roland Oberhänsli [2]

[1] Geology department, Faculty of earth science, Shahid Chamran University of Ahvaz, Ahvaz, Iran
[2] Institute of Earth and Environmental Sciences, Potsdam University, Karl-Liebknecht-Strasse 24, 14476 Potsdam, Germany

ARTICLE INFO

Submitted: April 2020
Accepted: March 2021
Available on line: July 2021

* Corresponding author:
adel_saki@scu.ac.ir

Doi: 10.13133/2239-1002/16632

How to cite this article:
Saki A. et al. (2021)
Period. Mineral. 90, 325-340

ABSTRACT

Precambrian meta-pelites of the Poshtuk area in northwest Iran contain the prograde mineral assemblage staurolite-garnet-chloritoid-muscovite-biotite that was replaced by the assemblage garnet-staurolite-chlorite-muscovite-biotite at peak metamorphic condition.

Whole-rock compositions reveal that high Fe, Al and Mn contents of their protolith rendered them prone to form these assemblages. Pseudosections calculated in KFMASH, MnKFMASH, and MnNCKFMASHO systems were used to investigate the P-T evolution of the samples. They clearly show the significant effect of MnO on the stability of the chloritoid-bearing assemblages and the formation of garnet through consumption of chlorite and chloritoid. The pseudosection in a T- aH_2O diagram shows that the studied assemblage could be stable only at a_{H2O}>0.8. X_{Mg} isopleths for garnet and biotite point to peak P-T conditions of about 3.75 kbar and 575 ºC. Chloritoid stability is overstepped with such conditions. This can be attributed to thermal perturbation due to plutonism. It is concluded, metamorphism was primarily controlled by advective heat from magmatic intrusions in the Poshtuk area. The Precambrian basement complexes were extensively overprinted by the Pan-African Orogeny as well as younger magmatic and metamorphic activities associated to Alpine Orogeny during convergence of Arabian and Eurasian plate.

Keywords: meta-pelites; pseudosection; chloritoid stability; Precambrain; Poshtuk

INTRODUCTION

The Iran microplate can be divided to several tectonic zones including Central Iran, Alborz, Zagros, Sanandaj-Sirjan, Urumieh-Dokhtar, Sistan and Makran (e.g. Stöklin, 1968; Sengör, 1984; Berberian and King, 1981; Alavi, 1994; Ghasemi and Talbot, 2006) (Figure 1a). The Mahneshan Metamorphic Complex (MMC) is located in NW Iran, SW of the Zanjan province (Figure 1a) and belongs to the Central Iran Zone. The continental crust of this zone was metamorphosed, intruded by granites and faulted during the Late Precambrian Pan-African Orogeny (Ramezani and Tucker, 2003). The study area is one of the remnants of the Precambrian terrane in Iran (Figure 1a). The MMC hosts a Precambrian-Cambrian crustal section containing schist, gneiss, granulite, amphibolite, and marble intruded by granite bodies. The metamorphic rocks of the MMC represent one of the best cases to investigate the lithological diversity and P-T evolution of this Precambrian metamorphic terrane. Calc-silicates of the MMC were studied by Moazzen et al. (2009). Hajialioghli et al. (2007) investigated the meta-ultramafic rocks. The meta-pelitic rocks include garnet andalusite schists, garnet staurolite schists, and chloritoid staurolite garnet schists (Saki et al., 2009; Saki

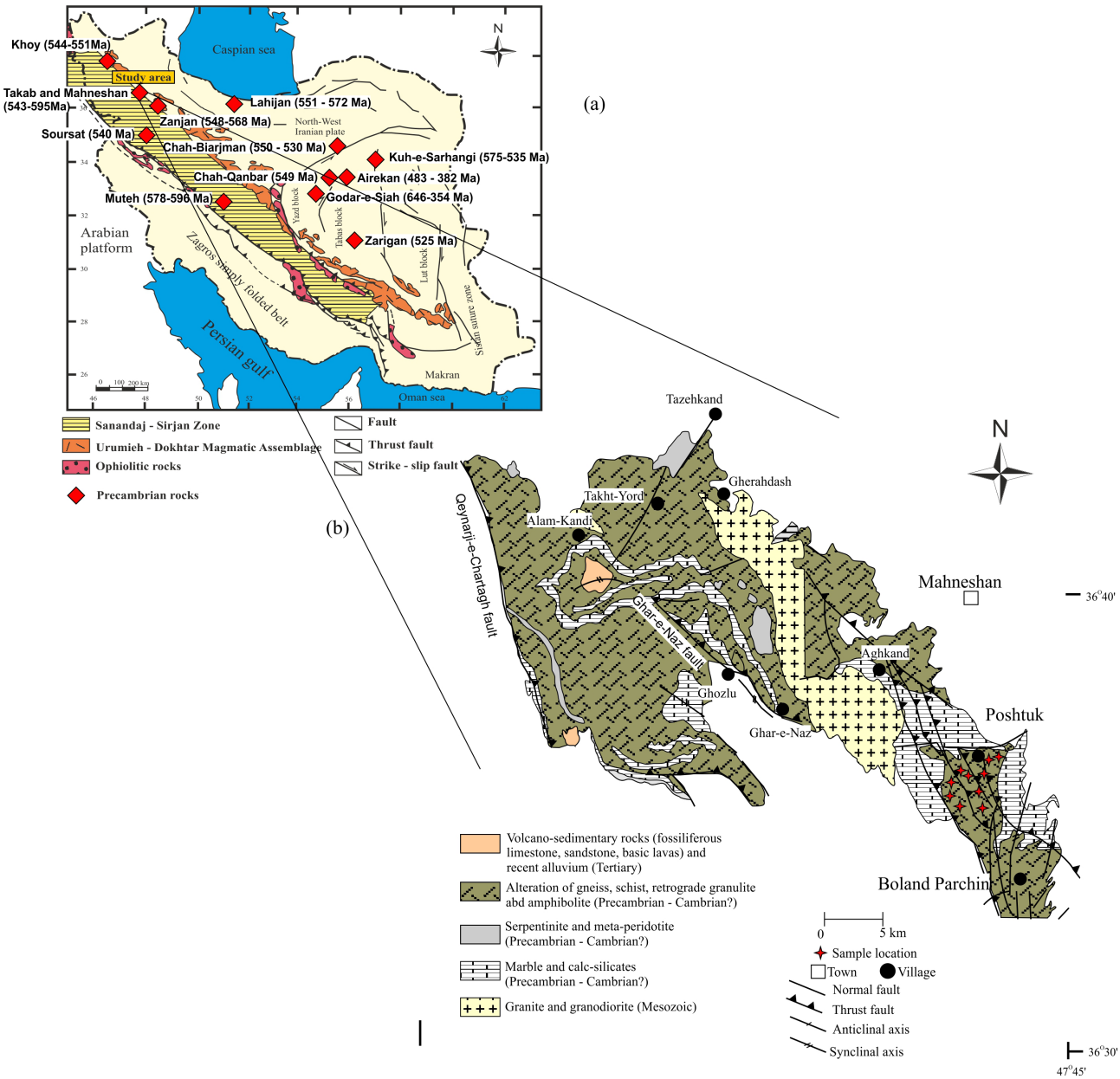

Figure 1. a) Geological map of Iran (Ghasemi and Talbot, 2006) with locations of the most important Precambrian granites and their U-Pb ages (after Shirdashtzadeh et al., 2018); b) geological map of the Maneshan area (after Babakhani and Ghalamghash, 1990; Saki, 2010) with sample locations.

et al., 2010; Saki et al., 2012). The chloritoid bearing schists occur only in the Poshtuk area in the southern part of the MMC (Figure 1b).

Saki et al. (2009) reported peak metamorphism assemblages of garnet+sillimanite+biotite+muscovite+quartz for chloritoid-free schists and garnet+staurolite+chlorite+muscovite+chloritoid+quartz (without biotite) for chloritoid bearing schists. Microscopic studies of new samples revealed the relatively rare assemblage staurolite-garnet-chloritoid-chlorite-muscovite-biotite pointing to peak metamorphic conditions. The assemblage is not ubiquitous and a few studies have investigated its formation condition and stability (e.g. Hoschek, 1969; Baltatzis, 1979; Hiroi, 1983; Bickle and Archibald, 1984; Wang and Spear, 1990; Droop and Harte, 1995; Sengupta, 2012). In the present paper, we try to explain the formation of this assemblage in the Poshtuk area meta-pelites using pseudosections and mineral-chemistry.

We also investigate the effect of MnO and H_2O activity on the stability of chloritoid-bearing assemblages and garnet in these samples.

GEOLOGICAL SETTING

The study area is mainly built by Neoproterozoic metamorphic rocks comprising schist, gneiss, marble, amphibolite, meta-diorite, meta-peridotite and serpentinite (Figure 1b). These are fine to medium-grained, strongly foliated greenschist to upper amphibolite facies rocks formed by convergence of the Arabian (Gondwana) and Turan (Eurasian) plates during the Pan-African Orogeny (Nadimi, 2007). The rocks have been thrust over Oligocene-Miocene volcano-sedimentary units along the NW-SE trending Qeynarj-e-Chartagh thrust fault and are unconformably overlain by Tertiary rocks in the east of the area (Babakhani and Ghalamghash, 1990). The Neoproterozoic complex was intruded by Ediacaran-Cambrian (531-576 Ma) granitoids, now gneiss, and Late Oligocene (25.41±0.4 Ma) biotite granites (Honarmand et al. 2018). According to Saki (2010) Neoproterozoic S-type granites formed during Pan-African orogeny due to anatexis. Ramezani and Tucker (2003) associated Cretaceous to Early Tertiary magmatism in Central Iran to the subduction of Neo-Tethys beneath Iranian microplate. Saki et al. (2012) also argued that the Early Tertiary magmatism caused multiple contact metamorphic events in the regional metamorphic rocks.

With respect to the unconformity between the metamorphosed Neoproterozoic - Early Cambrian rocks and large thick dolomitic marbles interlayered with volcanoclastic and volcanic rocks (corresponding to deepwater, turbiditic environments), it can be inferred that there was an arc-trench system along the Proto-Tethyan margin in NW Iran (Babakhani and Ghalamghash, 1990; Hajialioghli et al., 2007; Saki, 2010). Rapid exhumation of the basement rocks during Early Miocene (20 Ma) has been inferred from K-Ar dating of carbonaceous schists in the Zarshuran area (Mehrabi et al., 1999), apatite U-Th/He data from the Mahneshan area (Stockli et al., 2004) and ^{40}Ar-^{39}Ar dating of muscovite schists (Gilg et al., 2006). Hajialioghli et al. (2007) considered the meta-ultramafic rocks of the MMC as remnants of obducted Proto-Tethyan oceanic lithosphere. They estimated 410-540 ºC at X_{CO2}>0.1 for the metamorphism of these rocks. Moazzen et al. (2009) assessed 740 ºC and 8-9 kbar for peak and ~600 ºC and ~6 kbar for retrograde conditions for the calc-silicate rocks in the area.

Saki et al. (2010) estimated 600-620ºC and ~7 kbar for prograde (Barrovian-type) and 520-560 ºC and 2.5-3.5 kbar for retrograde metamorphism of aluminosilicate-bearing meta-pelites in the MMC. A clockwise P-T path characteristic of the metamorphic evolution of convergent/collisional orogenic belts was deduced. Saki et al. (2012) suggested 580 ºC and 3-4 kbar as peak metamorphic condition for staurolite-chloritoid schists from the Poshtuk area. They attributed the high T - low P metamorphism in this part of the MMC to the Early Tertiary magmatic activities. In the field, the biotite, garnet and staurolite isograds are difficult to distinguish as these minerals occur almost together, although a chloritoid-out isograd clearly separates the chloritoid-bearing and chloritoid-free rocks.

PETROGRAPHY

Based on petrographic studies, the following associations can be recognized in the samples: (1) Cld+St+Gt+Chl+Ms, (2) Cld+St+Gt+Chl+Ms+Bi and (3) St+Gt+And+Chl+Ms+Bi. The association (2) is relatively rare and occurs mostly in southern parts of the area. The flakes of biotite and muscovite define a prominent schistosity in the chloritoid-free schists (association 3) that wraps around garnet porphyroblasts (Figure 2a). In chloritoid-bearing schists (associations 1 and 2), fine lath-shaped chloritoids define the main foliation S_1 (the axial planar) (Figure 2 b-f). S_1 might develop simultaneously with the first generation of folds in the area (Saki et al., 2012). Chloritoid is in equilibrium with chlorite, muscovite and biotite along the foliation (Figure 2c). The subhedral to euhedral syntectonic garnet porphyroblasts grow over S_1 and commonly contain minute chloritoid inclusions (Figure 2d). Staurolite, the most abundant ferromagnesian mineral in the samples, occurs as anhedral to subhedral crystals of varying size (0.3 to 8 mm) (Figure 2 e,f). Staurolite is post-tectonic relative to the chlorite+chloritoid+muscovite assemblage and marks the S1 fabric. It replaces chloritoid and chlorite during prograde metamorphism. According to Saki et al. (2012), contact metamorphism in the area is characterized by formation of staurolite porphyroblasts in the regional metamorphic rocks. Biotite and magnetite apparently grow in equilibrium with staurolite. It can be inferred that these minerals constitute a paragenetic sequence and biotite would be a by-product of staurolite and chloritoid forming reactions (see below). The assemblage staurolite+garnet+chloritoid+chlorite+muscovite+biotite was replaced by staurolite+garnet+biotite+muscovite in chloritoid-free schists.

METAMORPHIC REACTIONS

To produce the assemblage staurolite+garnet+ chloritoid +chlorite+muscovite+biotite+magnetite a succession of low to medium grade reactions is needed. Chloritoid is the first Al-rich porphyroblastic phase to appear in meta-pelites and mostly forms from chlorite and muscovite consuming reactions at T>400 ºC (Thompson, 1976; Spear, 1993; Water and Lovegrove, 2002):

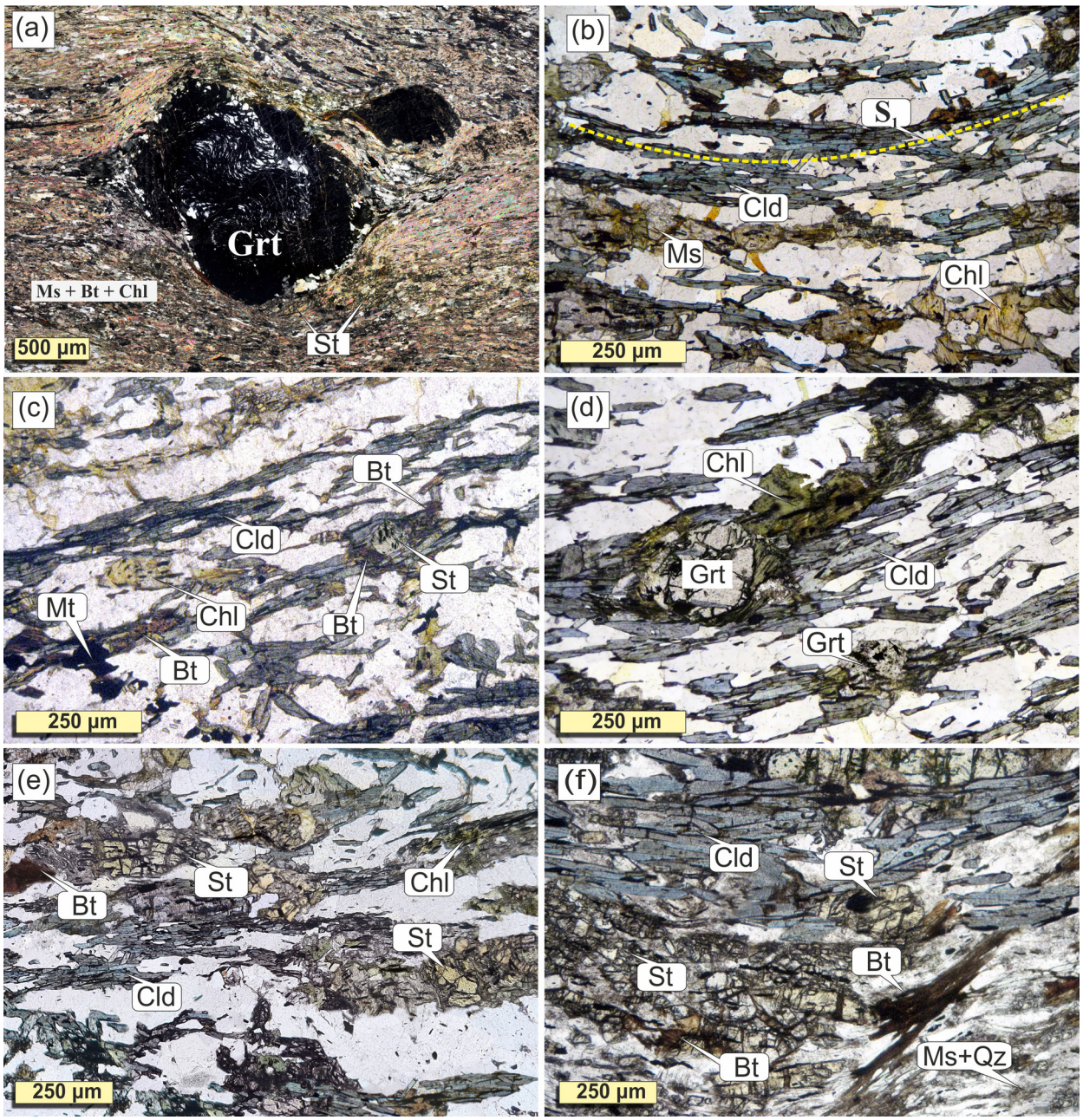

Figure 2. Photomicrograph of the samples. (a) Helicitic garnet porphyroblast in a matrix consisting of muscovite, chlorite, and biotite (XPL); (b) and (c) Perfectly aligned chloritoids and muscovites defining the schistosity (S_1); (d) Garnet growth in expense of chloritoid and chlorite bands; (e) and (f) Staurolite and biotite replacing chloritoid and chlorite bands in the studied samples. Mineral abbreviations: Bt=biotite; Chl=chlorite; Cld=chloritoid; Gt=garnet; Ms=muscovite; Mt=magnetite; St=staurolite (Whitney and Evans, 2010).

Fe-chlorite+hematite→chloritoid+magnetite+quartz +H_2O (1)

muscovite+chlorite→chloritoid+biotite+quartz+H_2O (2)

Since low-grade phyllites contain more chlorite than hematite, reaction 1 consumes all the hematite and forms the assemblage chlorite+chloritoid+magnetite. Reaction 2 could produce biotite, however, this is not a common phase in high Al-meta-pelites. The assemblage chloritoid+chlorite+muscovite was replaced by staurolite and garnet at higher temperatures through the following reactions (Thompson, 1976; Baltatzis, 1979; Wang and Spear, 1991; Spear, 1993):

chloritoid+chlorite+muscovite= staurolite+biotite+quartz $+H_2O$ (3)

chloritoid+ muscovite+quartz=staurolite+garnet+biotite $+H_2O$ (4)

chloritoid+quartz=staurolite+garnet+H_2O (5)

chlorite+chloritoid+ quartz=garnet+H_2O (6)

Formation of garnet and staurolite overprinting chloritoid and chlorite lathes (Figure 2) implies the occurrence of these reactions. Reactions 3 and 4 produce staurolite, garnet, and biotite simultaneously at similar P-T conditions. In Ca-poor meta-pelites, biotite associated with chloritoid is unstable at upper greenschist facies conditions (Bushmin and Glebovitsky, 2008) and can be replaced by garnet, and new muscovite and chlorite by the following reaction (Wang and Spear, 19991; Sengupta, 2012):

chloritoid+biotite+quartz=garnet+chlorite+muscovite $+H_2O$ (7)

This can explain dominance of muscovite and chlorite over biotite. The staurolite-garnet-chlorite assemblage is stable after complete breakdown of chloritoid (e.g. Spear, 1993).

ANALYTICAL METHODS

Major and trace elements were analyzed using a X-ray fluorescence (XRF) instrument model Philips PW 1480 XRF spectrometer at GeoForschungsZentrum (GFZ), Potsdam, Germany.

Chemical compositions of biotite, chloritoid, muscovite, staurolite, garnet, and plagioclase were determined by wavelength-dispersive spectrometry using a Cameca SX100 electron probe micro-analyzer (EPMA) system with accelerating voltage of 15 kV and 10-20 nA specimen current at the GeoForschungsZentrum (GFZ), Potsdam, Germany. Counting time on peaks was set to 10-30 s and 5-15 s on backgrounds, respectively. Analytical spot diameter was set between 3 and 5 μm. Natural and synthetic standards were used for calibration.

WHOLE ROCK CHEMISTRY

Chemical compositions of the Poshtuk area chloritoid staurolite garnet schists are given in Table 1. All samples are rich in SiO_2 (56.5 to 61.2 wt%), Al_2O_3 (18.3 to 23 wt%) and FeO (10.5 to 12.9 wt%). K_2O (1.72 to 3.51 wt%) is higher than Na_2O (0.4 to 1.56 wt%). The samples plot mostly in the field of Fe-rich shale on a log $Fe_2O_3(t)/K_2O$ vs. log SiO_2/Al_2O_3 discrimination diagram (Figure 3). They also contain some CaO (0.5 to 1.6 wt%) indicating minor contents of carbonate minerals in the protolith.

MINERAL CHEMISTRY

Staurolite

Table 2 shows the chemical composition of four representative staurolite samples. The structural formulae were calculated according to 46 oxygen atoms. Staurolite is Fe-rich (Fe total=3.31 to 3.48 apfu) and no chemical zoning is observed.

Chloritoid

Chloritoid analyses are represented in Table 2. The formulae were calculated based on 6 oxygen atoms. Chloritoid is rich in Al and Fe with Mg# of about 0.89.

Table 1. Chemical composition of the chloritoid bearing schists from the Poshtuk area.

Sample	P-1	P-2	P-3	P-4	P-5	P-6	average
SiO_2	60.00	56.50	56.60	61.20	59.98	58.60	58.81
TiO_2	0.88	0.79	1.09	1.16	1.13	0.78	0.97
Al_2O_3	18.30	23.00	20.50	19.10	21.01	19.80	20.29
$Fe_2O_3(t)$	10.50	11.75	10.65	12.88	12.62	10.65	11.51
MnO	0.10	0.35	0.31	0.25	0.38	0.25	0.27
MgO	2.26	1.28	1.90	1.10	1.08	2.00	1.60
CaO	1.29	1.04	2.20	0.48	0.48	1.61	1.18
Na_2O	1.56	0.58	1.09	0.40	0.39	1.48	0.92
K_2O	3.51	2.86	3.62	1.76	1.72	2.49	2.66
P_2O_5	0.18	0.12	0.14	0.06	0.06	0.15	0.12
Total	98.58	98.27	98.10	98.40	98.86	97.80	98.33
LOI	1.22	1.50	1.90	1.48	1.11	1.85	1.51

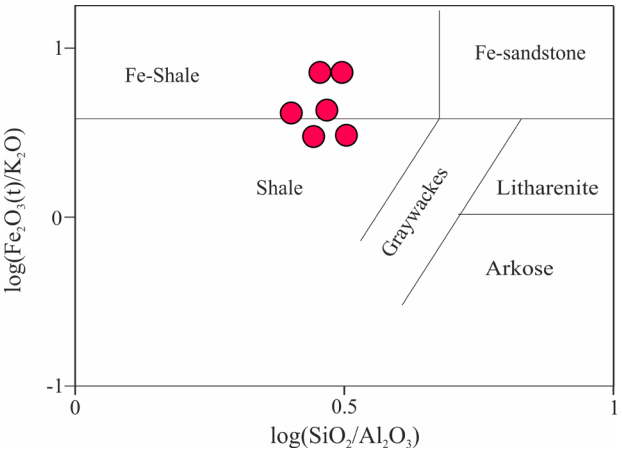

Figure 3. log $Fe_2O_3(t)/K_2O$ versus log SiO_2/Al_2O_3 discrimination diagram (Herron, 1988) for the studied samples. The samples mostly plot in the field of Fe-shales.

Figure 3a, shows its composition of on Fe-Mn-Mg and $Al+Fe^{+3}$-Fe^{+2}+Mn-Mg triangular diagrams.

Garnet

Chemical compositions of cores and rims of three representative garnet crystals are given in Table 3. The garnet formulae were calculated on the basis of 12 oxygen atoms. Garnet is rich in Fe with almandine ranging from 0.83 to 0.85. No significant chemical zoning is observed despite a minor increase of Mn from rim to core. Similarly, Baltatzis (1979) reported that garnet in the chloritoid and chloritoid+staurolite zones are not chemically zoned or its zonation is minimal. All points plot in the almandine field on a Mg-Fe-Ca classification diagram (Figure 3b).

Biotite

Representative analyses of biotite are listed in Table 2. For use in geothermometric calculations, we analyzed biotite in equilibrium with garnet. The formulae were calculated based on 11 oxygen atoms. Biotite is rich in FeO (23.9 to 24.8 wt%) and plots as annite in the Fe^{+2}+Mn+Ti-Al^{VI} (*feal*) vs Mg-Li (*mgli*) classification diagram (Tischendorf et al., 2007) (Figure 3c). The Mg# ($Mg/Fe^{+2}+Mg$) ranges from 0.32 to 0.34.

Muscovite

The chemical compositions of four representative muscovites are given in Table 2. The chemical formula of white mica, following the scheme proposed in Marrone et al. (2020), was calculated on the basis of 11 oxygens (e.g., Parra et al., 2002) and ∑ (Si, Al, Ti, Cr, Mn, Mg, Fe)=6.01 cations, assuming Fe^{3+}=[9.98-2*(Si+Ti)-(Al+Cr)-2*(Ca+Ba)-(Na+K)], and a stoichiometric fixed trioctahedral substitution (XTri=0.01). The molar fractions of paragonite (XPg=atomic [Na/(Na+K+Ca+Ba)]), pyrophyllite (XPrl=[1-(Na+K+Ca+Ba)]), muscovite (XMs=Al[IV]-{XPg+XPrl+(XTri/2)+Ti+(Fe3+/2)+[(Ca+Ba)/(Na+K+Ca+Ba)]}) and celadonite (XCel =1-{XMs+XPg+XPrl+(XTri/2)+Ti+[(Ca+Ba)/(Na+K+Ca+Ba)]}) were then calculated. Phengite content (XPh) is then assumed as the sum of XMs+XCel. The muscovite is rich in Al and K and plots in the field of muscovite in the Fe+2+Mn+Ti-AlVI (feal) vs Mg-Li (mgli) classification diagram (Tischendorf et al., 2007) (Figure 3c). Na/(Na+K) continents (0.22 in average) indicates paragonite end-member components. The phengite contents range 0.71 to 0.74.

Chlorite

Representative analyses of chlorite in contact with biotite are listed in Table 2. The formulae were calculated on the basis of 14 oxygen atoms. Chlorite is rich in FeO (35.4 to 39 wt%) and Al_2O_3 (22.8 to 23.1 wt%) and plots in the field of pseudothuringit in a Si vs. Fe_{total} classification diagram (Hey, 1954) (Figure 4d).

Plagioclase

Table 2 represents the chemical compositions of the plagioclase. Plagioclase are rich in Na_2O (8.1 to 8.3 wt%) relative to CaO (4.6 to 5.7 wt%) and their X_{Ab} and X_{An} range from 0.7 to 0.76 and from 0.23 to 0.27, respectively. No significant chemical zoning was observed, however rims are slightly richer in anorthite component.

GEOTHERMOBAROMETRY

Saki et al. (2012) used the garnet-chloritoid geothermometer and multiple-equilibrium calculations to estimate P-T condition of staurolite-chloritoid schists from the Poshtuk area. We used the garnet-biotite geothermometer (e.g. Dasgupta et al., 1991; Holdway, 2000) to account for the presence of garnet and biotite. Biotite, garnet and plagioclase showing equilibrium textures were used for calculations. The calculations show a temperature range of 540 to 610 ºC.

The garnet-biotite-plagioclase-quartz (GBPQ) (Wu et al., 2004) geobarometer was used to estimate the pressure. It is applicable for aluminosilicate bearing/free meta-pelites at metamorphic conditions from 515 to 778 ºC and 1 to 11 kbar. Moreover, X_{An}>0.17 in plagioclase, $X_{Grossular}$>0.3 in garnet and X_{Al}>0.3 of biotite (X_{Al}=Al/Al+Fe+Mg+Ti) render the results reliable (Wu et al., 2004). GBPQ delivered 2.9 to 4.5 kbar (3.9 on average) for the Poshtuk chloritoid staurolite garnet schists.

PSEUDOSECTIONS

Three pseudosections for the systems KFMASH, MnKFMASH, and MnNCKFMASHO were calculated

Table 2. Representative chemical compositions of minerals from the Poshtuk area chloritoid-bearing schist. Ferric iron contents is calculated on stoichiometric criteria (Droop, 1987). The major element oxides are given in wt%.

	Chloritoid				Biotite				Chlorite				Staurolite			
SiO_2	23.84	23.91	23.68	24.07	36.17	36.04	36.4	36.6	22.77	22.92	22.69	22.52	27.21	28.00	27.95	27.41
TiO_2	0.00	0.02	0.01	0.00	1.26	0.91	1.05	1.22	0.08	0.22	0.11	0.14	0.52	0.70	0.66	0.42
Al_2O_3	40.94	40.85	40.69	41.35	17.29	17.47	16.97	16.63	22.97	23.09	23.11	22.86	56.91	56.29	56.00	56.80
Cr_2O_3	0.07	0.06	0.04	0.07	0.02	0.30	0.05	0.02	0.06	0.07	0.08	0.09	0.05	0.06	0.04	0.03
Fe_2O_3	2.72	3.31	3.99	2.74	0.00	0.00	0.00	0.00	2.69	2.14	1.87	2.04	0.81	0.81	0.81	0.81
FeO	25.51	25.56	24.4	25.77	23.91	24.41	24.85	24.08	36.75	35.43	37.83	39.09	13.79	14.30	14.62	14.40
MnO	0.03	0.00	0.99	0.03	0.01	0.07	0.00	0.03	0.09	0.07	0.07	0.12	0.07	0.15	0.15	0.16
MgO	1.62	1.67	1.62	1.63	7.03	7.27	6.92	6.63	7.06	8.11	6.50	5.49	0.32	0.30	0.31	0.33
CaO	0.01	0.02	0.00	0.01	0.01	0.00	0.01	0.03	0.00	0.00	0.00	0.01	0.00	0.01	0.00	0.01
Na_2O	0.00	0.01	0.00	0.00	0.17	0.01	0.14	0.2	0.04	0.01	0.01	0.02	0.00	0.02	0.01	0.00
K_2O	0.02	0.00	0.01	0.02	9.55	9.23	9.41	9.74	0.01	0.01	0.00	0.00	0.01	0.00	0.01	0.01
Totals	94.76	95.41	95.43	95.69	95.42	95.71	95.8	95.18	92.52	92.06	92.32	92.38	99.69	100.64	100.56	100.38
Si	0.97	0.97	0.96	0.97	2.81	2.79	2.83	2.86	4.90	4.90	4.91	4.90	7.41	7.57	7.58	7.44
Ti	0.00	0.00	0.00	0.00	0.07	0.05	0.06	0.07	0.01	0.04	0.02	0.02	0.11	0.14	0.14	0.09
Al	1.97	1.96	1.95	1.97	1.58	1.60	1.55	1.53	5.81	5.84	5.89	5.88	18.27	17.94	17.89	18.17
Cr	0.00	0.00	0.00	0.00	0.00	0.02	0.00	0.00	0.00	0.00	0.00	0.00	0.01	0.01	0.01	0.01
Fe^{+3}	0.08	0.10	0.12	0.08	0.00	0.00	0.00	0.00	0.00	0.00	0.00	0.00	0.17	0.16	0.17	0.17
Fe^{+2}	0.87	0.87	0.83	0.87	1.55	1.58	1.61	1.57	7.21	6.80	7.24	7.56	3.14	3.23	3.31	3.27
Mn	0.00	0.00	0.03	0.00	0.00	0.01	0.00	0.00	0.02	0.01	0.01	0.02	0.02	0.03	0.03	0.04
Mg	0.10	0.10	0.10	0.10	0.81	0.84	0.80	0.77	2.26	2.58	2.09	1.78	0.13	0.12	0.13	0.13
Ca	0.00	0.00	0.00	0.00	0.00	0.00	0.00	0.00	0.00	0.00	0.00	0.00	0.00	0.00	0.00	0.00
Na	0.00	0.00	0.00	0.00	0.03	0.00	0.02	0.03	0.03	0.01	0.01	0.02	0.00	0.01	0.01	0.00
K	0.00	0.00	0.00	0.00	0.95	0.91	0.93	0.97	0.01	0.01	0.00	0.00	0.00	0.00	0.00	0.00
Sum	4.00	4.00	4.00	4.00	7.81	7.80	7.81	7.81	20.25	20.19	20.17	20.19	29.26	29.23	29.26	29.31

C: core, R: rim, Alm: Almandine; Adr: Andradite, Grs: Grossularite, Prp: Pyrope, Sps: Spessartine, Ab: Albite, An: Anorthite, Or: Orthoclase, Mg# = $(Mg/Mg+Fe^{+2})$. (a) White mica molar fractions: XPrl: Pyrophyllite, XTri: Trioctahedral substitution, XPg: Paragonite, XCel: Celadonite; XMs: Muscovite. Trioctahedral substitution is fixed by stochiometry at XTri=0.01. (b) Phengite: XPh: (XMs + XCel).

to investigate the effects of MnO and other components on the stability of the assemblage staurolite+garnet+chloritoid+chlorite+muscovite+biotite+magnetite (Figures 5 and 6). They were calculated using Theriak/Domino software version 04.02.2017 (de Capitani and Petrakakis, 2010) with an internally consistent thermodynamic dataset of Holland and Powell (1998). An average bulk composition of the samples (Table 1) was used for calculations. LOI was considered as pure H_2O fluid. TiO_2 was excluded because muscovite, biotite, and chlorite contain only very small amounts of TiO_2 (Tables 2 and 3) and the samples lack ilmenite. Wei and Powell (2004) report that the exclusion of TiO_2 has no significant effect on phase diagrams.

The KFMASH and MnKFMASH system pseudosections are represented in Figure 5. The stability of the chloritoid-bearing assemblages differs in these pseudosections (shaded areas in Figure 5). In the KFMASH system (Figure 5a), chloritoid-bearing stability fields are mostly limited to the temperatures below 530 ^oC. Lack of MnO prevents formation of spessartine in low-grade fields. Therefore, garnet appears for the first time at 590 ^oC and pressures higher than 4.5 kbar. No stability field containing chloritoid+garnet is obvious. This is due to a large temperature gap (~90 ^oC) between the reactions chloritoid-out and garnet-in, implying that garnet could

Table 2. ...Continued

	Garnet 1		Garnet 2		Garnet 3			Muscovite				Plagioclase			
	C	R	C	R	C	R									
SiO_2	36.55	36.85	36.36	36.76	36.28	36.72		45.60	45.80	46.05	46.26	61.94	62.48	62.64	61.01
TiO_2	0.10	0.06	0.10	0.07	0.07	0.14		0.18	0.20	0.18	0.19	0.00	0.00	0.01	0.00
Al_2O_3	21.27	20.14	20.53	20.78	21.18	20.13		38.24	37.96	37.90	37.42	25.22	25.29	24.31	25.60
Cr_2O_3	0.00	0.00	0.00	0.00	0.00	0.00		0.03	0.00	0.05	0.00	0.00	0.00	0.00	0.00
Fe_2O_3	0.08	1.29	1.00	0.49	0.52	1.45		0.00	0.00	0.00	0.00	0.00	0.00	0.00	0.00
FeO	37.67	37.99	37.14	37.98	37.96	38.50		1.55	1.50	1.51	1.48	0.14	0.12	0.13	0.07
MnO	1.39	0.96	1.71	0.74	1.55	0.65		0.00	0.01	0.00	0.01	0.07	0.05	0.08	0.00
MgO	1.70	2.30	1.78	2.26	1.46	2.34		0.18	0.27	0.28	0.26	0.02	0.01	0.02	0.00
CaO	1.95	1.37	2.09	1.43	2.16	1.27		0.01	0.00	0.00	0.00	4.57	5.03	4.63	5.74
Na_2O	0.00	0.00	0.00	0.00	0.00	0.00		1.84	1.81	1.64	1.79	8.20	8.28	8.27	8.13
K_2O	0.00	0.00	0.00	0.00	0.00	0.00		9.11	9.10	8.69	8.97	0.28	0.31	0.35	0.30
Totals	100.55	101.07	101.98	101.85	102.29	101.84		96.73	96.64	96.29	96.38	100.44	101.57	100.44	100.85
Si	2.96	2.98	2.95	2.98	2.94	2.97		2.97	2.98	2.99	3.02	2.73	2.72	2.76	2.69
Ti	0.01	0.00	0.01	0.00	0.00	0.01		0.01	0.01	0.01	0.01	0.00	0.00	0.00	0.00
Al	2.03	1.93	1.97	1.99	2.02	1.92		2.93	2.91	2.90	2.88	1.31	1.30	1.26	1.33
Cr	0.00	0.00	0.00	0.00	0.00	0.00						0.00	0.00	0.00	0.00
Fe^{+3}	0.01	0.08	0.06	0.03	0.03	0.09		0.08	0.08	0.08	0.08	0.00	0.00	0.00	0.00
Fe^{+2}	2.55	2.57	2.52	2.57	2.57	2.60		0.00	0.00	0.00	0.00	0.01	0.00	0.00	0.00
Mn	0.10	0.07	0.12	0.05	0.11	0.04		0.00	0.00	0.00	0.00	0.00	0.00	0.00	0.00
Mg	0.20	0.28	0.22	0.27	0.18	0.28		0.02	0.03	0.03	0.03	0.00	0.00	0.00	0.00
Ca	0.17	0.12	0.18	0.12	0.19	0.11		0.00	0.00	0.00	0.00	0.22	0.23	0.22	0.27
Na	0.00	0.00	0.00	0.00	0.00	0.00		0.23	0.23	0.21	0.23	0.70	0.70	0.71	0.69
K	0.00	0.00	0.00	0.00	0.00	0.00		0.76	0.76	0.72	0.75	0.02	0.02	0.02	0.02
Sum	10.57	10.67	10.62	10.62	10.64	10.72	[a]XPrl	0.01	0.02	0.07	0.03	4.99	4.99	4.98	5.01
Alm	84.13	84.51	82.54	84.96	83.99	85.28	[a]XTri	0.01	0.01	0.01	0.01	0.02	0.02	0.02	0.02
Adr	0.26	3.95	3.11	1.51	1.63	3.70	[a]XPg	0.23	0.23	0.21	0.23	0.75	0.74	0.75	0.71
Grs	5.46	0.40	3.05	2.65	4.75	0.00	[a]XCel	0.00	0.01	0.01	0.04	0.23	0.25	0.23	0.28
Prp	6.93	9.30	7.31	9.16	6.00	9.52	[a]XMs	0.75	0.74	0.70	0.70	-	-	-	-
Sps	3.22	2.21	3.99	1.71	3.63	1.50						-	-	-	-
Mg#	0.07	0.10	0.08	0.10	0.06	0.10	[b]XPh	0.75	0.75	0.71	0.74	-	-	-	-

C: core, R: rim, Alm: Almandine; Adr: Andradite, Grs: Grossularite, Prp: Pyrope, Sps: Spessartine, Ab: Albite, An: Anorthite, Or: Orthoclase, Mg# = $(Mg/Mg+Fe^{+2})$. (a) White mica molar fractions: XPrl: Pyrophyllite, XTri: Trioctahedral substitution, XPg: Paragonite, XCel: Celadonite; XMs: Muscovite. Trioctahedral substitution is fixed by stochiometry at XTri=0.01. (b) Phengite: XPh: (XMs + XCel).

not form through the chloritoid consuming reactions (3) to (6). This is not consistent with our microscopic observations.

Many studies have shown the effect of MnO on the stability of garnet, chloritoid, staurolite and cordierite during metamorphism (e.g. Atherton, 1964; Kramm, 1973; Wang and Spear, 1991; Tinkham et al., 2001; White et al., 2014). This effect is clear from the MnKFMASH

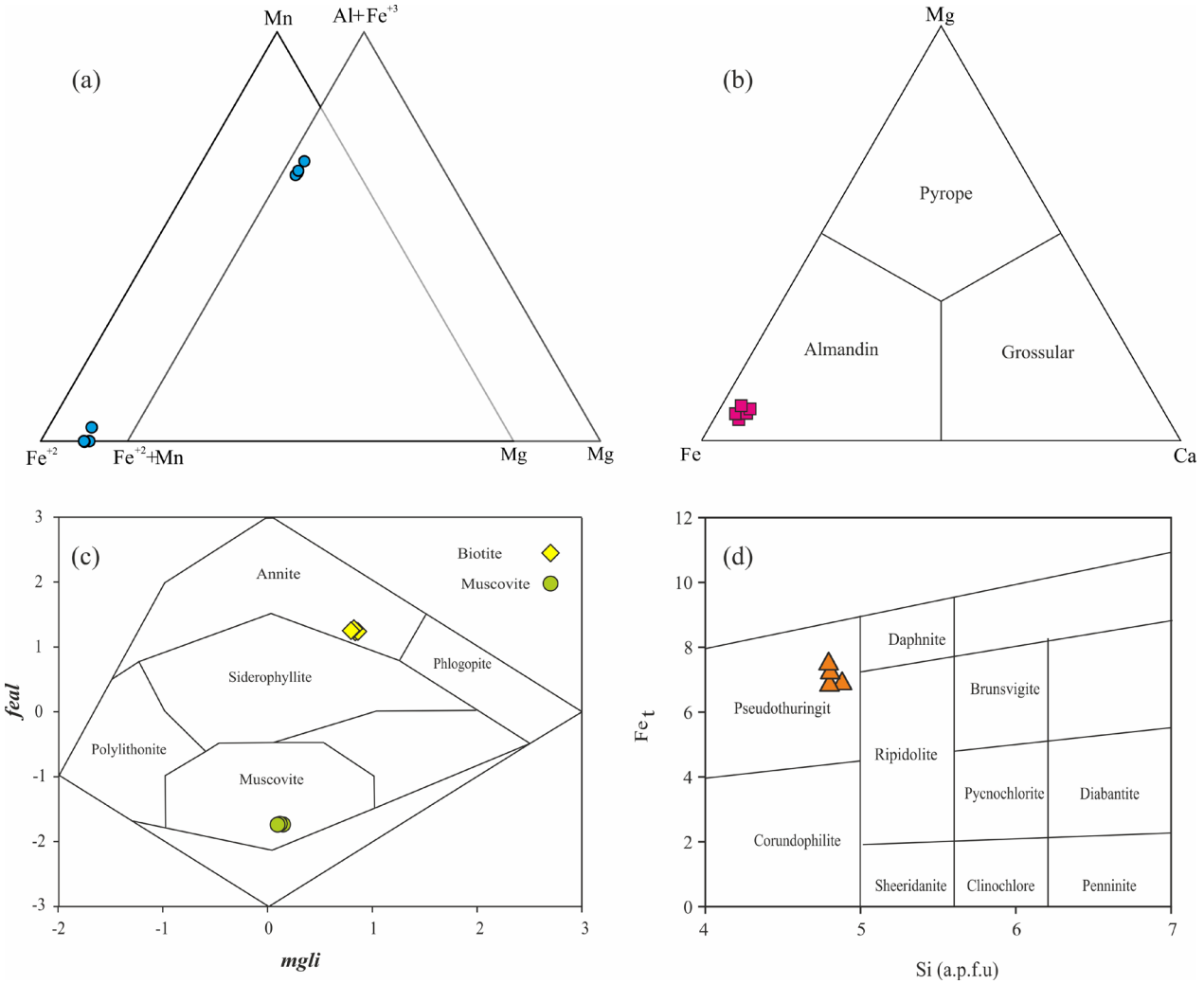

Figure 4. a) Chemical composition of chloritoid on Fe-Mn-Mg and Al+Fe^{+3}-Fe^{+2}+Mn-Mg triangular diagrams; b) Fe-Mg-Ca classification diagram (Grew et al., 2013) for garnet. All the analyzed points (cores and rims) plot in almandine field; c) Fe^{+2}+Mn+Ti-Al^{VI} (*feal*) vs Mg-Li (*mgli*) classification diagram (Tischendorf et al., 2007) for muscovite and biotite; d) composition of chlorite on $Fe_{(t)}$ vs Si classification diagram (Hey, 1954).

pseudosection (Figure 5b). The addition of MnO to the KFMASH system shifts the stability of chloritoid bearing assemblages to higher temperatures by about 40 ºC. The garnet stability field extends to 530 ºC and 3kbar, P-T conditions lower than in the KFMASH system (Figure 5a). Garnet with high spessartine content appears. The high almandine content of garnet in the samples restricts formation in such condition. The pseudosection also predicts the replacement of chloritoid by garnet with rising temperature.

To consider all minerals in our samples, a MnNCKFMASHO pseudosection was calculated (Figure 6). Mg#(MgO/MgO+FeO), X_{Alm}-, X_{prp}- and X_{Mg}- isopleths for garnet and biotite were calculated and represented in Figure 6. The new system provides plagioclase and margarite (at high P) and increases the stability of chloritoid slightly (~10 ºC). The equilibrium assemblage staurolite+garnet+chloritoid+chlorite+muscovite+biotite observed by microscope and determined by microprobe analysis is constricted to a narrow temperature range of 530 to 570 ºC at 3 to 6 kbar (the yellow colored area in Figure 6a). According to the diagram, chloritoid drops out of this system at higher P-T conditions as compared to the former (Figure 5b). The position of the average estimated P-T (blue circle) point to higher PT conditions. This indicates that the observed assemblage is either not an equilibrium assemblage or significant overstepping for chloritoid must be postulated.

The calculated isopleths for biotite and garnet allow to further constrain the P-T conditions for the Poshtuk

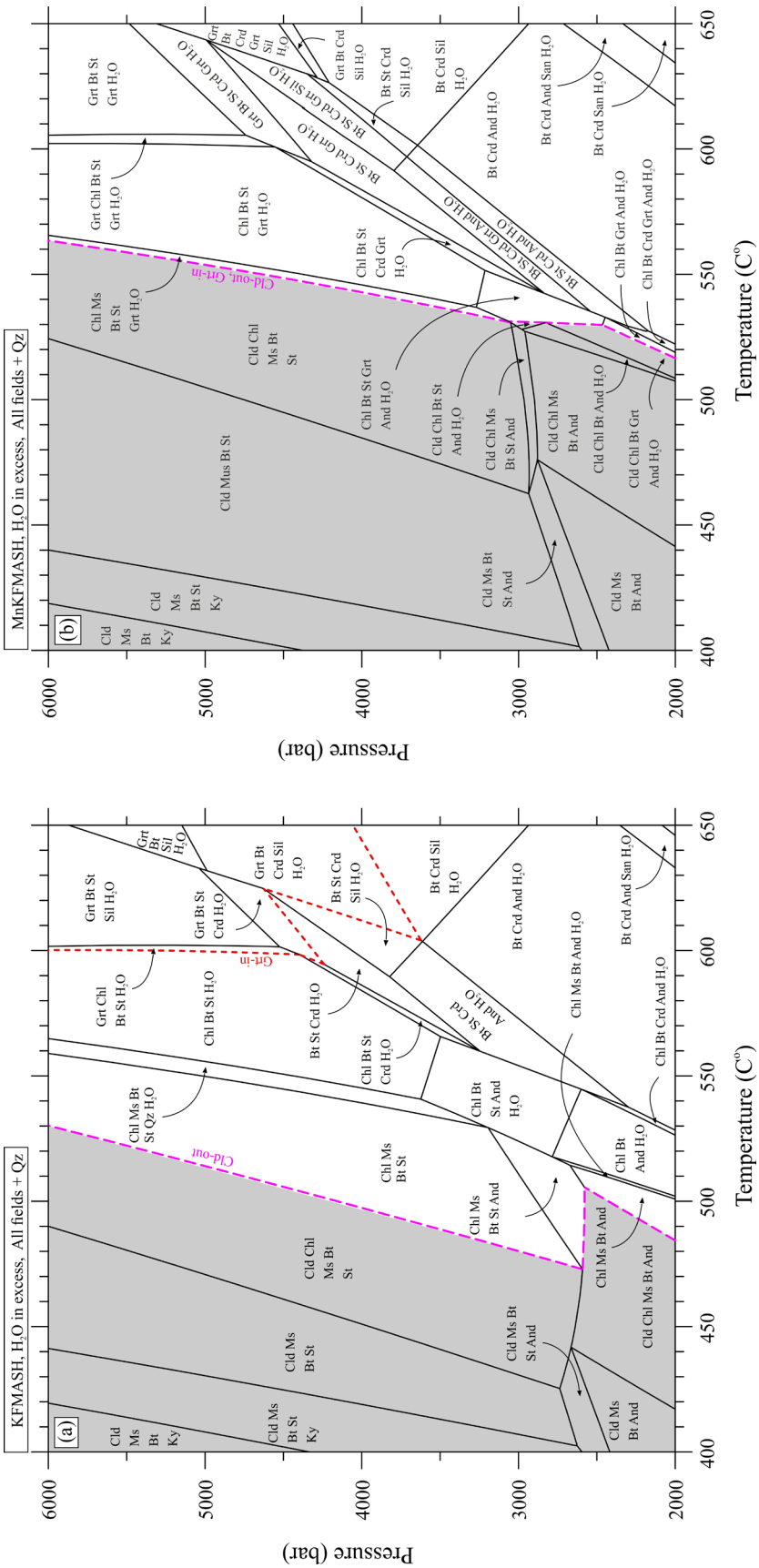

Figure 5. Pseudosections calculated using Theriak/Domino software version 04.02.2017 (de Capitani and Petrakakis, 2010) on (a) KFMASH and (b) MnKFMASH system with H_2O in excess. The shaded areas show the stability fields of chloritoid-bearing assemblages. Mineral abbreviations: And=andalusite; Bt=biotite; Chl=chlorite; Cld=chloritoid; Crd=cordierite; Grt=garnet; Ms=muscovite; Mt=magnetite; San=sanidine; Sil=sillimanite; St=staurolite (Whitney and Evans, 2010).

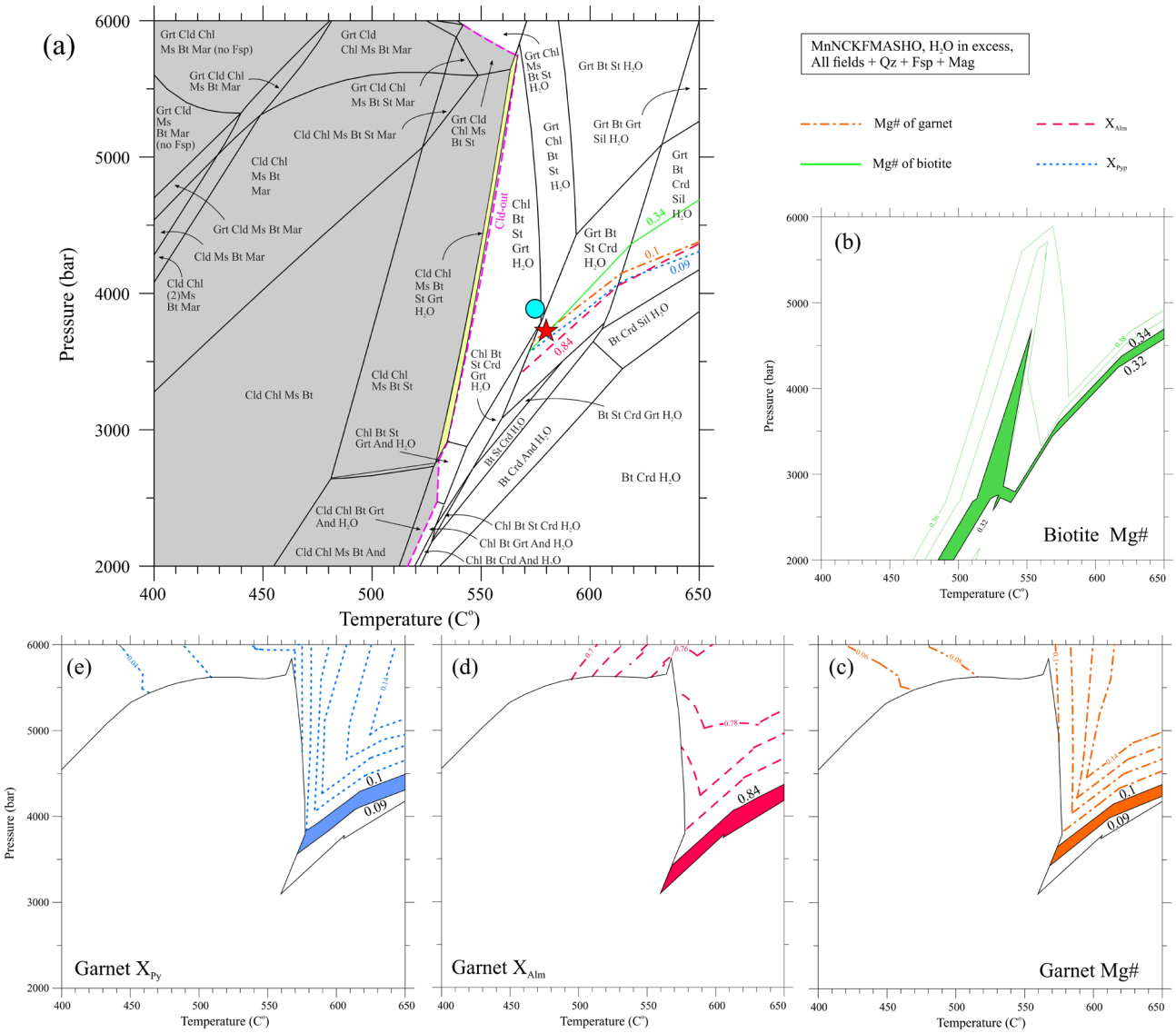

Figure 6. a) Pseudosection calculated for the MnNCKFMASHO system with H_2O excess. The shaded area shows the stability of chloritoid bearing assemblages; b and c) Mg# (Mg/Mg+Fe^{+2}) isopleths for garnet and biotite; d and e) X_{Alm}-, X_{prp}- isopleths for garnet. The blue circle shows average estimated P-T for the samples and the red star shows the intersection of garnet and biotite Mg# isopleths. Mineral abbreviations: And=andalusite; Bt=biotite; Chl=chlorite; Cld=chloritoid; Crd =cordierite; Fsp=feldspar; Gt=garnet; Mar=margarite, Mt=magnetite; Ms=muscovite; Mt=magnetite; San=sanidine; Sil=sillimanite; St=staurolite (Whitney and Evans, 2010).

assemblage. The Mg# isopleths for garnet and biotite range from 0.04 to 0.14 and 0.32 to 0.44, respectively, with higher values correlating to higher temperatures. Also, X_{Alm}- and X_{prp}- isopleths of garnet range from 0.62 to 0.84 and 0.04 to 0.14, respectively. Considering the calculated Mg# [Mg/(Mg+Fe^{+2})] of about 0.1 for garnet (rim) and 0.34 for biotite (Table 2), the Mg# isopleths intersect at ~575 °C and 3.75 kbar. The calculated X_{Alm} (0.84) is slightly lower than the measured values (0.85 on average, Table 2) and does not fit the intersection point, although intersecting with the X_{prp}- isopleth (0.09) at about 600 °C and 4 kbar (the red star in Figure 6a). These P-T conditions are consistent with the geothermobarometric calculations (section 7) and the values reported by Saki et al. (2012) for the staurolite-chloritoid schist of the Poshtuk area, but outside the stability field of chloritoid in Figure 6. Thus, due to the high amount of chloritoid, it might have survived by overstepping its stability field of a system with pure H_2O during prograde metamorphism in the Poshtuk area.

The fluid composition is important for the formation and stability of metamorphic assemblages. In the pseudosection, we assumed the fluid to be pure H_2O. However regarding the CaO contents of the samples (Table 1), the effect of other fluid constitutes such as CO_2 must be considered. To investigate the effect of H_2O activity on the formation of the Poshtuk assemblage, we calculated a H_2O activity versus temperature (aH_2O-T) pseudosection at 4 kbar (Figure 7). As visible, the mineral assemblages change with different aH_2O. Chloritoid occurs at aH_2O ranging from 0.25 to 1 and temperatures below 550 ºC. At low temperatures (450 ºC for example), staurolite and biotite are stable only at low aH_2O (~0.25 to 0.53) but their stability fields expand with rising temperatures. On the other hand, chlorite and muscovite are present only at aH_2O higher than 0.4 and garnet occurs in various fields from low to high aH_2O. The assemblage staurolite+garnet +chloritoid+chlorite+muscovite+biotite appears at aH_2O of about 0.83 to 1 and in a very narrow temperature range of about 530 to 545 ºC. The aH_2O amount is in good agreement with the results obtained by Saki et al. (2012) for the staurolite-chloritoid schist of the study area and shows that CO_2 had effect on the formation of the studied assemblage.

DISCUSSION

In general, meta-pelites containing the assemblage staurolite+garnet+chloritoid+chlorite+muscovite+biotite are relatively rare. Some authors have studied similar assemblages (e.g. Hoschek, 1969; Baltatzis, 1979; Hiroi, 1983; Bickle and Archibald, 1984; Wang and Spear, 1990; Droop and Harte, 1995; Sengupta, 2012). Meta-pelites containing chloritoid + biotite have been reported from low-pressure (<7 kbar) terranes (e.g. Harte and Hudson, 1979; Wang and Spear, 1990; Droop and Harte, 1995; Sengupta, 2012). According to Droop and Harte (1995) and Bushmin and Glebovitsky (2008), a chloritoid+biotite zone is generally absent from typical Barrovian sequences (medium pressures) and, when present, can only be found in aluminous rocks. Wang and Spear (1991) report that the formation of a chloritoid+biotite paragenesis is rather controlled by bulk composition than by P-T conditions and this paragenesis forms in meta-pelites containing Fe/(Mg+Fe+Mn)> ~0.6. Previous studies have shown that chloritoid+biotite+staurolite occurs mostly in Fe and Al-rich meta-pelites (e.g. Baltatzis, 1979; Hiroi, 1983; Waters and Lovegrove, 2002). Most of these studies estimated 480 to 550 ºC and 3 to 6 kbar for peak conditions (e.g. Hoschek, 1969; Baltatzis, 1979; Hiroi, 1983; Bickle and Archibald, 1984; Wang and Spear, 1990; Droop and Harte, 1995; Sengupta, 2012). Hoschek (1969) argued that chloritoid+biotite associations are stable only within a small temperature range in the upper greenschist facies. Wang and Spear (1991) demonstrated that chloritoid+biotite parageneses are stable over a wide range of P-T conditions. It is worth to note that, according to Sengupta (2012), the garnet+chloritoid+biotite+chlorite±magnetite assemblage becomes unstable at low aH_2O and when H_2O concentration is diluted, stability of garnet+chlorite is preferred over chloritoid+biotite.

Based on the above arguments, the chemical composition of the Poshtuk area meta-pelite (Table 1; Fe/(Mg+Fe +Mn)=0.82-0.9, Fe_2O_3=10.5-12.88 and Al_2O_3= 18.3-23) was suitable to form the paragenesis staurolite +garnet+chloritoid+biotite. A relatively pure H_2O fluid provided the proper conditions for the stability of that assemblage. According to microscopic observations, chloritoid+chlorite+muscovite can be considered as the low-grade assemblage for the samples at T>400 ºC. Biotite was probably absent, as Al-rich meta-pelites do not contain biotite at low grade (Tinkham et al., 2001). At higher grades, biotite, garnet, and staurolite formed at the expense of the chloritoid, chlorite and muscovite through the reactions (3) to (6). These reactions simultaneously formed staurolite and garnet at lower amphibolite facies P-T conditions. On the other hand, higher modal amounts of staurolite than garnet point to the importance of reaction (3) during formation of the studied assemblage. In meta-pelites with high Al_2O_3 contents, staurolite occurs before garnet at the expense of chloritoid (White et al., 2014). Moreover, Mn-bearing staurolites can form earlier than garnet in chloritoid bearing rocks (Hiroi, 1983; White et al., 2014). In the pseudosections (Figures 5 and 6) the chloritoid+biotite+chlorite+staurolite assemblage is stable prior to the formation of the first garnet.

The estimated P-T conditions through geothermo-barometry and isopleths intersection (Figure 6) are both higher than the stability fields defined for chloritoid in previous studies (e.g. Hoschek, 1969; Baltatzis, 1979; Hiroi, 1983; Bickle and Archibald, 1984; Wang and Spear, 1990; Droop and Harte, 1995; Sengupta, 2012). This indicates overstepping of chloritoid stability limits in the Poshtuk meta-pelites. Chloritoid to staurolite overstepping has been studied by Pattison et al. (2011) who attributed this to a combination of some factors such as low reaction affinity of chloritoid consuming reactions, difficulty of staurolite nucleation and slow dissolution rate of chloritoid. These factors cause a metastable breakdown of chloritoid and its higher thermal stability. According to Hollister (1969), short time-scale intrusions with small-scale thermal metamorphic events can cause significant over-stepping. Waters and Lovegrove (2002) report that this is more likely due to rock composition, reaction sequence and growth mechanisms. Other factors such as strain energy (Pattison et al., 2011; Spear et al., 2014) and presence of fluid (Pattison and Thinkham,

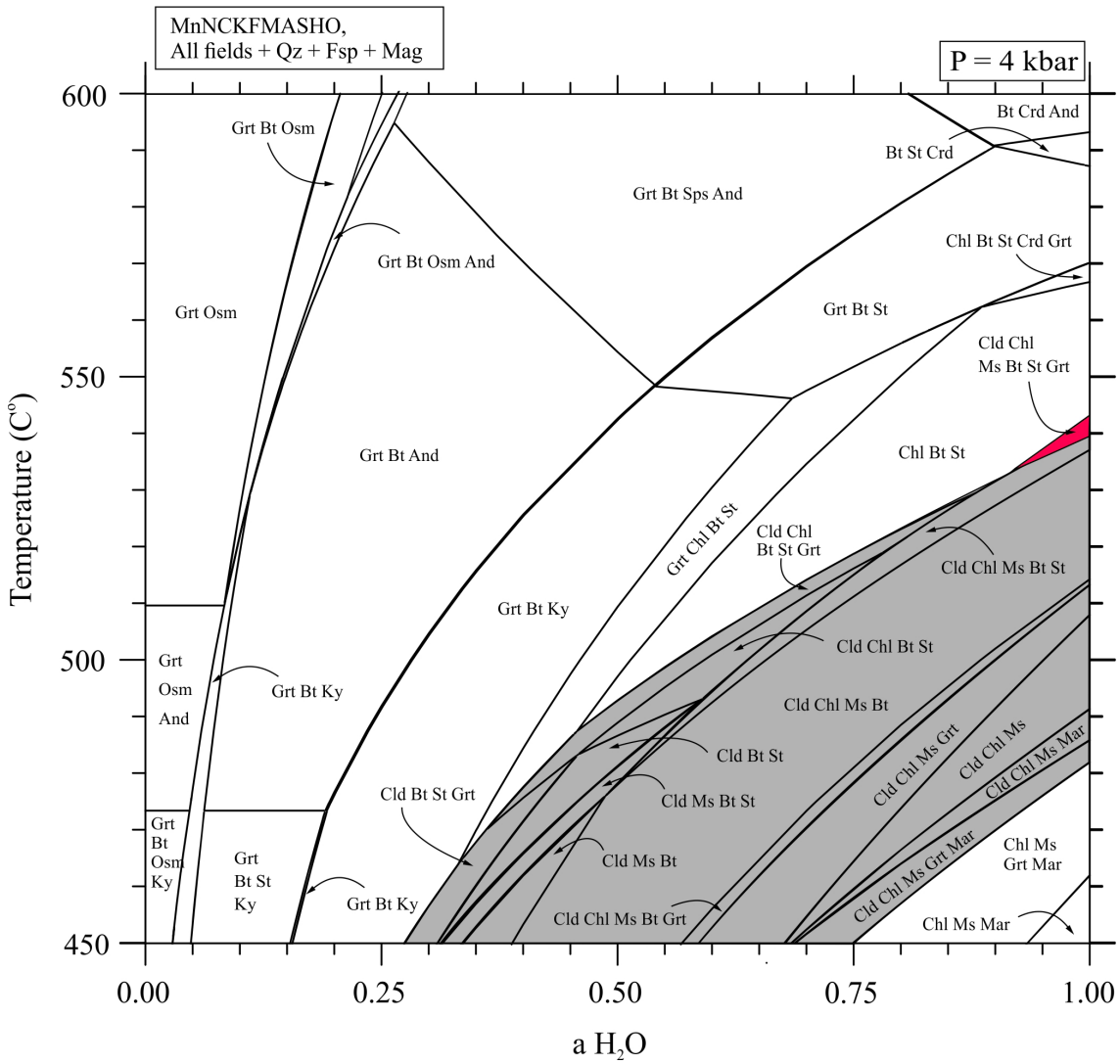

Figure 7. T- aH_2O pseudosection for a MnNCKFMASHO system. The shaded area shows the stability of chloritoid bearing assemblages. The red-colored area indicates stability of the staurolite+garnet+chloritoid+chlorite+muscovite+biotite assemblage.
Mineral abbreviations: And=andalusite; Bt=biotite; Chl=chlorite; Cld=chloritoid; Crd=cordierite; Fsp=feldspar; Gt=garnet; Mar=margarite, Mt=magnetite; Ms=muscovite; Mt=magnetite; San=sanidine; Sil=sillimanite; St=staurolite (Whitney and Evans, 2010).

2009) could similarly cause mineral over-stepping. All of the mentioned factors can be considered for the Poshtuk meta-pelites regarding their geological background including strong deformation and several intrusions of granitoid bodies in the area. Formation of the peak metamorphic assemblage staurolite+garnet+chloritoid+ biotite is due to contact metamorphism (Saki, 2010; Saki et al., 2012) inferring that thermal shocks and the presence of magmatic fluids were the most effective factors for overstepping of the chloritoid stability field in the meta-pelites. The MnO content of the protolith, as discussed earlier, lets chloritoid be stable over a wide range of temperature. According to Pattison and Spear (2018) deformation reduces kinetic barriers for nucleation. Thus, lack of deformation during contact metamorphism would render nucleation of staurolite and garnet difficult and retain the stability of chloritoid. Here, low reaction rates of chloritoid consumption is not to be considered for the over-stepping as the rates rise with increasing temperature (e.g. Baxter, 2002; Llana-Fúnez et al., 2012).

CONCLUSIONS

Calculated pseudosections for the chloritoid staurolite garnet schists from the Poshuk area (NW Iran) in KFMASH, MnKFMASH, and MnNCKFMASHO systems show a significant effect of MnO, Al_2O_3 and

FeO on the stability of chloritoid-bearing assemblages. The calculated X_{Mg} isopleths for garnet and biotite give peak P-T conditions of about 575 ºC and 3.75 kbar. Under such P-T condition, chloritoid was overstepping its stability field due to the intrusion of igneous bodies, their associated fluids and diminution in nucleation of staurolite and garnet. The aH_2O vs T pseudosection demonstrates that the assemblage staurolite+garnet+chloritoid+chlorite +muscovite+biotite is stable in $aH_2O>0.8$. Thus, H_2O was not a pure fluid in the system and contribution of other components such as CO_2, F and S (originated from magmatic fluids) should be considered. Intrusion of granitoid bodies into the Precambrian basement in NW Iran during Tertiary controlled peak metamorphic conditions and formation of the assemblage staurolite+ chloritoid+garnet+ biotite in the Poshuk meta-pelites.

ACKNOWLEDGEMENTS

This research is supported by Shahid Chamran University of Ahvaz (Grant No. SCU.EG98.44295). We wish to thank Dr. Gilles Chazot and Dr. Leonardo Casini for their constructive comments. The authors are deeply grateful to Dr. Federico Lucci for his generous advices and helps.

REFERENCES

Alavi M., 1994. Tectonics of the Zagros orogenic belt of Iran: new data and interpretations. Tectonophysics 229, 211-38.

Atherton M.P., 1964. The garnet isograd in pelitic rocks and its relationship to metamorphic facies. American Mineralogist 49, 1331-1349.

Babakhani A.R. and Ghalamghash J., 1990. Geological map of Takht-e-Soleiman, 1:100,000, Geological Survey of Iran, Tehran.

Baltatzis E., 1979. Staurolite-Forming Reactions in the Eastern Dalradian Rocks of Scotland. Contributions in Mineralogy and Petrology 69, 193-200.

Baxter E.F., 2002. Natural constraints on metamorphic reaction rates. Geological Society, London, Special Publications 220, 183-202.

Berberian M. and King G.C., 1981. Towards a paleogeography and tectonic evolution of Iran. Canadian Journal of Earth Sciences 18, 210-65.

Bickle M.J. and Archibald N.J., 1984. Chloritoid and staurolite stability: implications for metamorphism in the Archaean Yilgarn Block, western Australia. Journal of Metamorphic Geology 2, 179-203.

Dasgupta S., Sengupta P., Guha D., Fukuoka M., 1991. A reined garnet-biotite Fe- Mg exchange geothermometer and its application in amphibolites and granulites. Contribution to Mineralogy and Petrology 109, 130-137.

de Capitani C. and Petrakakis K., 2010. The computation of equilibrium assemblage diagrams with Theriak/Domino software. American Mineralogist 95, 1006-1016.

Droop G.T.R., 1987. A general equation for estimating Fe^3 concentrations in ferromagnesian silicates and oxides from microprobe analyses using stoichiometric criteria. Mineralogical Magazine 51, 431-5.

Droop G.T.R. and Harte B., 1995. The effect of Mn on the phase relations of medium grade pelites: constraints from natural assemblages on petrogenetic grid topology. Journal of Petrology 36, 1549-1578.

Droop G.T.R. and Jahangiri A., 2009. Peak and post-peak P-T conditions and fluid composition for scapolite clinopyroxene-garnet calc-slicate rocks from the Takab area, NW Iran. European Journal of Mineralogy 21, 149-162.

Ghasemi A. and Talbot C.J., 2006. A new tectonic scenario for the Sanandaj-Sirjan Zone (Iran). Journal of Asianan Earth Sciences 26, 683-693.

Gilg H.A., Boni M., Balassone G., Allen C.R., Banks D., Moore F., 2006. Marble-hosted sulfide ores in the Angouran Zn-(Pb-Ag) deposit, NW Iran: interaction of sedimentary brines with a metamorphic core complex. Mineralium Deposita 41, 1-16.

Grew E., Locock A., Mikks S.J., Galuskina I.O., Galuskin E.V., Halenius U., 2013. Nomenclature of the garnet supergroup. American Mineralogist 98, 785-811.

Hajialioghli R., Moazzen M., Droop G.T.R., Oberhänsli R., Bousquet R., Jahangiri A., Ziemann M., 2007. Serpentine polymorphs and P-T evolution of metaperidotites and serpentinites in the Takab area, NW Iran. Mineralogical Magazine 71, 203-222.

Harte B. and Hudson N.F.C., 1979. Pelitic facies series and the temperatures and pressures of Dalradian metamorphism in eastern Scotland. In: The Celadonides of the British Isles: Reviewed. (Eds.) A.L. Harris, C.H. Holland, B.E. Leake, Geological Society Special Publications, London, 323-337.

Herron M.M., 1988. Geochemical classification of terrigenous sands and shales from core or log data. Journal of Sedimentary Petrology 58, 820-829.

Hey M.H., 1954. A new review of the chlorites. Mineralogical Magazine 30, 277-292.

Hiroi Y., 1983. Progressive Metamorphism of the Unazuki Pelitic Schists in the Hida Terrane, Central Japan. Contributions to Mineralogy and Petrology 82, 334-350.

Holdaway M.J., 2000. Application of new experimental and garnet Margules data to the garnet-biotite geothermometer. American Mineralogist 85, 881-892.

Holland T. and Powell R., 1998. An internally consistent thermodynamic data set for phases of petrological interest. Journal of Metamorphic Geology 16, 309-343.

Honarmand M., Xiao W., Nabatian G., Blades M.L., dos Santos M.C., Collins A.S., Ao S., 2018. Zircon U-Pb-Hf isotopes, bulk-rock geochemistry and Sr-Nd-Pb isotopes from late Neoproterozoic basement in the Mahneshan area, NW Iran: Implications for Ediacaran active continental margin along the northern Gondwana and constraints on the late Oligocene

crustal anatexis. Gondwana Research 57, 48-76.

Hoschek G., 1969. The stability of staurolite and chloritoid and their significance in metamorphism of pelitic rocks. Contributions to Mineralogy and Petrology 22, 208-232.

Kramm U., 1973. Chloritoid Stability in Manganese Rich Low-Grade Metamorphic Rocks, Venn-Stavelot Massif, Ardennes, Contributions to Mineralogy and Petrology 41, 179-196.

Llana-Fúnez S., Wheeler J., Faulkner D.R., 2012. Metamorphic reaction rate controlled by fluid pressure not confining pressure: implications of dehydration experiments with gypsum. Contributions to Mineralogy and Petrology 164, 69-79.

Marrone S., Monié P., Rossetti F., Lucci F., Theye T., Bouybaouene M.L., Zaghloul M.N., 2020. The Pressure-Temperature-time-deformation history of the Beni Mzala unit (Upper Sebtides, Rif belt, Morocco): Refining the Alpine tectono-metamorphic evolution of the Alboran Domain of the Western Mediterranean, Journal of Metamorphic Geology, https://doi.org/10.1111/jmg.12587.

Mehrabi B., Yardley B.W.D., Cann J.R., 1999. Sediment-hosted disseminated gold mineralization at Zarshuran, NW Iran. Mineralium Deposita 34, 673-696.

Moazzen M., Oberhänsli R, Hajialioghli R., Möller A., Bousquet R., Droop G.T.R., Jahangiri A. 2009. Peak and post-peak P-T conditions and fluid composition for scapolite-clinopyroxene-garnet calcsilicate rocks from the Takab area, NW Iran. European Journal of Mineralogy 21, n149-62.

Nadimi A., 2007. Evolution of the Central Iranian basement. Gondwana Research 12, 324-333.

Parra T., Vidal O., Jolivet L., 2002. P-T path of high-pressure, low-temperature schists on Tinos Island (Cyclades Archipelago, Greece) using chlorite-potassic white mica pairs. Lithos 63, 41-66.

Pattison D.R.M. and Tinkham D.T., 2009. Interplay between equilibrium and kinetics in prograde metamorphism of pelites: an example from the Nelson aureole, British Columbia. Journal of Metamorphic Geology 27, 249-279.

Pattison D.R.M., De Capitani C., Gaidies F., 2011. Petrological consequences of variations in metamorphic reaction affinity. Journal of Metamorphic Geology 29, 953-977.

Pattison D.R.M. and Spear F., 2018. Kinetic control of staurolite-Al_2SiO_5 mineral assemblages: Implications for Barrovian and Buchan metamorphism, Journal of Metamorphic Geology 36, 667-690.

Ramezani J. and Tucker R.D., 2003. The Saghand region, central Iran: U-Pb geochronology, petrogenesis and implications for Gondwana tectonics. American Journal of Science 303, 622-665.

Saki A., 2010. Proto-Tethyan remnants in northwest Iran: Geochemistry of the gneisses and metapelitic rocks. Gondwana Research 17, 704-71.

Saki A., Moazzen M., Oberhänsli R., 2012. Mineral chemistry and thermobarometry of the staurolite-chloritoid schists from Poshtuk, NW Iran. Geological Magazine 149, 1077-1088.

Saki A., Moazzen M., Modjtahedi M., Oberhänsli R., 2009. Phase relations and reaction histories of chloritoid-free and chloritoid-bearing meta-pelites from the Mahneshan area, NW Iran. Iranian Journal of Crystallography and Mineralogy 16, 622-640.

Sengör A.M.C., 1984. The Cimmeride orogenic system and tectonics of Eurasia. Geological Society of America, New York, 82 pp.

Sengupta N., 2012. Stability of chloritoid+biotite-bearing assemblages in some meta-pelites from the Palaeoproterozoic Singhbhum Shear Zone, eastern India and their implications. Geological Society Special Publications 365, 91-116.

Shirdashtzadeh N., Torabi G., Schaefer B., 2018. A magmatic record of Neoproterozoic to Paleozoic convergence between Gondwana and Laurasia in the northwest margin of the Central-East Iranian Microcontinent. Journal of Asian Earth Scineces 166, 35-47.

Spear F.S., 1993. Metamorphic Phase Equilibria and Pressure-Temperature-Time Paths. Mineralogical Society of America, Washington DC, 799 pp.

Stockli D.F., Hassanzadeh J., Stockli L.D., Axen G., Walker J.D., Dewane T.J., 2004. Structural and geochronological evidence for Oligo- Miocene intra arc low-angle detachment faulting in the Takab- Zanjan area, NW Iran. Geological Society of America Annual Meeting Denver, 319.

Stöcklin J., 1968. Structural history and tectonics of Iran: a review. American Association of Petroleum Geologists Bulletin 52, 1229-1258.

Thompson A.B., 1976. Mineral reactions in pelitic rocks; I. Prediction of P-T-X(Fe-Mg) phase relations. American Journal of Science 276, 401-424.

Tinkham D.K., Zuluaga C.A., Stowell H.H., 2001. Meta-pelite phase equilibria modeling in MnNCKFMASH: the effect of variable Al_2O_3 and Mg/(Mg+Fe) on mineral stability. Geological Materials Research 3, 1-42.

Tischendorf G., Förster H.J., Gottesmann B., Rieder M., 2007. True and brittle micas: composition and solid-solution series. Mineralogical Magazine 71, 285-320.

Wang P. and Spear F.S., 1991. A field and theoretical analysis of garnet+chlorite+chloritoid+biotite assemblages from the tri-state (MA, CT, NY) area USA. Contributions to Mineralogy and Petrology 106, 217-235.

Watersand D.J. and Lovegrove D.P., 2002. Assessing the extent of disequilibrium and overstepping of prograde metamorphic reactions in meta-pelites from the Bushveld Complex aureole, South Africa. Journal of Metamorphic Geology 20, 135-149.

Wei C.J. and Powell R., 2004. Calculated phase relations in high-pressure meta-pelites in the system NKFMASH (Na_2O-K_2O-FeO-MgO-Al_2O_3-SiO_2-H_2O) with application to natural rocks. Journal of Petrology 44, 183-202.

White R.W., Powell R., Johnson T.E., 2014. The effect of Mn on mineral stability in meta-pelites revisited: new *a-x* relations

for manganese-bearing minerals. Journal of Metamorphic Geology 32, 809-828.

Whitney D.L. and Evans B.W., 2010. Abbreviations for names of rock-forming minerals. American Mineralogist 95, 185-187.

Wu C.M., Zhang J., Ren L.D., 2004. Empirical garnet-biotite-plagioclase-quartz (GBPQ) geobarometry in medium- to high-grade meta-pelites. Journal of Petrology 45, 1907-1921.